Available online at www.sciencedirect.com
ScienceDirect
Journal of Magnetic Resonance 190 (2008) 142–148
JMR Journal of Magnetic Resonance
www.elsevier.com/locate/jmr

Communication

Fast (4,3)D GFT-TS NMR for NOESY of small to medium-sized proteins

Youlin Xia [a,*], Sudha Veeraraghavan [b], Qi Zhu [a], Xiaolian Gao [a]

[a] *Department of Biology and Biochemistry, University of Houston, Houston, TX 77004, USA*
[b] *Structural Biology Research Center, Department of Biochemistry & Molecular Biology, University of Texas – Houston Medical School, USA*

Received 24 May 2007; revised 16 September 2007
Available online 22 September 2007

Abstract

NOESY NMR spectra provide interproton distance information for a molecule in solution and the complete, unambiguous determination of NOESY spectral assignments is the basis for protein structure determination. High resolution NOESY can be obtained from ^{13}C and ^{15}N isotope edited four-dimensional (4D) data, but these experiments would normally require weeks to complete. We have applied a G-matrix Fourier transform and time-sharing (GFT-TS) NMR method for simultaneously acquiring two sets of 4D NOESY data. The implementation of the GFT-TS allows 2.5- to 5-fold reduction in experimental time without sacrificing spectral resolution as compared with that of 3D data. The ^{13}C, ^{15}N-edited GFT-TS (4,3)D H–N–*CN*–H NOESY (GFT dimensions are underlined and TS dimensions are in italics) provides convenient and unambiguous NOE assignments for HN/HN and HN/HC for a sample of 1.4 mM ubiquitin (76 amino acids, 8.5 kDa). We also provide a set of utility scripts for data processing and spectral assignment to facilitate the use of GFT NMR. This method shows great promise for routine high quality NMR NOESY data collection for small to medium sized proteins.

Keywords: GFT NMR; RD NMR; Time-sharing (TS); NOESY

Multi-dimensional nuclear magnetic resonance (MD NMR) spectroscopy has no doubt brought about a new age of biomolecular structure determination. NMR technology has been continuously evolving and now is a key driver for unveiling the function of proteins on a proteomic scale. Recently, several novel methods were put forward to achieve multidimensional NMR in shorter time and higher spectral resolution. PR NMR (PR-projection and reconstruction) data acquisition was proposed in 2003 and MD NMR data were acquired by cross peak reconstruction based on 2D orthogonal and tilted projections [1–3]. G-matrix NMR (GFT NMR) [4–8] is a successful application of NMR in reduced dimensions (RD NMR) [9–15]. By simultaneously acquiring multiple nuclear frequencies in the same evolution time period using a quadrature detection, GFT NMR was shown to allow reducing overall NMR time in a 5D bond-correlation NMR experiment by as many as 125-fold. In a sense, GFT NMR can be considered a sub-class of projection spectroscopy [16], as it produces convoluted data in projected dimensions. A single-scan NMR experiment acquires MD NMR data in one scan utilizing an echo-planar chemical shift imaging technique which contains spatially dependent evolutions and spatially discriminated detection [17]. All of these experiments apply to only scalar coupling connectivity assignments of nuclei. Several time-sharing (TS) methods have been demonstrated in TS 2D, 3D, and 4D experiments [18–23] and in a 2TS 3D NOESY experiment [24]. Using the TS or 2TS methods, experimental time can be saved by 50% or 75%, respectively, and multiple sets of data can be acquired in a single experiment. Besides the promising aspects of the above methods in improving the sensitivity and resolution of the homo- and hetero-nuclear MD NMR experiments, similar improvements in NOESY

* Corresponding author. Fax: +1 713 743 2636.
E-mail address: yxia@uh.edu (Y. Xia).

1090-7807/$ - see front matter © 2007 Elsevier Inc. All rights reserved.
doi:10.1016/j.jmr.2007.09.015

experiments for dipolar coupling measurements are highly desirable [25].

The measurements of ^1H–^1H connectivities (NOEs) constitute the basis of protein structure determination and the quality and the quantity of unambiguously determined NOEs determine both the precision and the accuracy of the resulting structures [26,27]. For moderate to large size proteins, NOEs are obtained from ^{15}N and/or ^{13}C-edited NOESY experiments [28–31] and it is most desirable that optimal spectral resolution be obtained. Thus, when possible, 4D NOESY would be the experiment of choice, since in these spectra, the proton resonances separated by either ^{13}C or ^{15}N provide unambiguous assignments. 4D NOESY, however, is obtained at a lower spectral resolution than that of the equivalent 3D NOESY due to experimental time restraints. The complete ^1H NOE assignments would require several 4D experiments to extract ^1H_C–^1H_C, ^1H_N–^1H_N, and ^1H_C–^1H_N (or ^1H_N–^1H_C) NOEs.

We believe that GFT NMR offers a solution to improve the conventional multidimensional NOESY. In a previous publication [7], we discussed the advantages of reducing one dimension from n to $n-1$ dimensions, such as (3,2)D GFT NMR heteronuclear correlation experiments, representing a good compromise of sensitivity (for mM protein samples), practical usefulness, and time-saving factors. We further consider that the GFT NMR may be used in combination with TS to reduce NMR experimental time without losing spectral resolution. Unlike the complicated data of a GFT-dimension, the TS NMR signal frequencies in the same dimension are represented separately as in the corresponding conventional multidimensional spectra.

We have applied a new GFT-TS NMR experiment, employing ^{13}C, ^{15}N-edited 4D NOESY in a reduced dimension, to illustrate an effective solution to the limitations discussed above. This (4,3)D H–N–*CN*–H NOESY experiment (GFT convoluted H and N dimensions underlined; time-shared C and N dimensions in italic) takes advantage of both GFT NMR and TS NMR to simultaneously acquire two equivalent sets of 4D NOESY, i.e., (4,3)D H–N–N–H and (4,3)D H–N–C–H NOESY, which were transformed into the corresponding 4D H–N–N–H and H–N–C–H NOESY with the data recovery operation. This experiment records ^{13}C and ^{15}N isotopically edited 4D ^1H_N–^1H_N and ^1H_N–^1H_C NOEs, allowing the ^1H_N and ^1H_C assignments through N–H and C–H bond connectivities, respectively. The (4,3)D H–N–*CN*–H NOESY experiment was completed in two days for the 1.4 mM ubiquitin protein, representing a 5-fold (2.5-fold) reduction in data acquisition time compared to the corresponding conventional 4D H–N–N–H and H–N–C–H NOESY experiments recorded using comparable parameters of acquisition, which would require ten days (five days) of experimental time (if the two 4D data are acquired in a time-shared mode for the F_3 dimension).

The GFT-TS (4,3)D H–N–*CN*–H NOESY pulse sequence is shown in Fig. 1. In this experiment, the evolutions of ^1H and ^{15}N spins before mixing time share the t_1 dimension in a manner of GFT NMR and the evolutions of ^{13}C and ^{15}N spins after mixing time share the t_2 dimension in a manner of TS NMR. Semi-constant-time evolution mode is applied in the t_1 dimension for ^1H_N frequency labelling to reduce signal decay. After the mixing

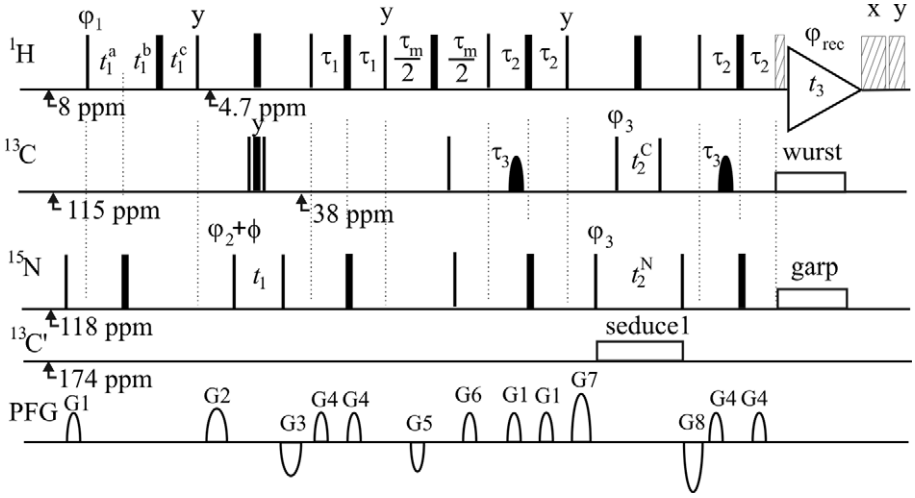

Fig. 1. Pulse sequence of (4,3)D H–N–*CN*–H NOESY. Narrow and wide bars represent 90° and 180° pulses, respectively. The spin lock pulse (1 ms) and x and y purge pulses (3 and 2 ms) were applied immediately before and after acquisition, respectively. The ^{13}C shape pulses were 200 μs G3 180° pulses. $\tau_1 = 2.6$ ms, $\tau_2 = 1.7$ ms, $\tau_3 = 1.6$ ms, $\tau_m = 200$ ms. Recovery delay between two scans was set to 1.0 s. Semi-constant time scheme was applied for ^1H evolution in t_1 dimension: $t_1^a(0) = \tau_1, t_1^b(0) = 3$ μs, $t_1^c(0) = t_1^a(0) + t_1^b(0)$; $\Delta t_1^a = 1/\text{sw1}$, $\Delta t_1^b = \Delta t_1^a - \Delta t_1^c$, $\Delta t_1^c = t_1^c/n1$ (sw1 and n1 are the spectral width and the number of complex points in t_1 dimension, respectively). For ^{13}C and ^{15}N simultaneous evolution times, t_2^C and t_2^N, half point delays were used. Default phases were x: $\phi = 0°$; $\varphi_1 = 2(x), 2(-x)$; $\varphi_2 = 4(x),4(-x)$; $\varphi_3 = (x, -x)$; $\varphi_r = (x, -x, -x,x, -x,x,x, -x)$. Quadrature detections in t_1 and t_2 were acquired via States-TPPI of φ_1 and φ_3, respectively. A second 3D data set was acquired via altering ϕ by 90°. The two sets of 3D data with $\phi = 0°$ and 90°, respectively, were acquired in an interleave mode and stored separately. The durations and strengths of the gradients are G1 = (1 ms, 15 G/cm); G2 = (1 ms, 8 G/cm); G3 = (1 ms, −20 G/cm); G4 = (1 ms, 6 G/cm), G5 = (1 ms, −10 G/cm), G6 = (1 ms, 10 G/cm), G7 = (3 ms, 25 G/cm), and G8 = (4 ms, −25 G/cm). For ^{15}N-singly labelled proteins, the pulses of ^{13}C should be removed so that (4,3)D H–N–N–H NOESY can be acquired.

time, a core double INEPT is employed for simultaneous ^1H_N and ^1H_C polarization transfers. The PFG G7 and G8 with opposite polarities and spin lock pulse and trim pulses are used to suppress water peaks for a sample of protein dissolved in H_2O. The J couplings between ^{13}CO and both ^{15}N and $^{13}C_\alpha$ are removed by the seduce1 decoupling sequence. In this experiment, two 3D data sets, S_1 and S_2, were acquired by altering the phase ϕ by 90°:

$$S_1 = 0.5[e^{i(\Omega_{HN'}+\Omega_{N'})t_1} + e^{i(\Omega_{HN'}-\Omega_{N'})t_1}] \times [e^{j\Omega_N t_2^N} e^{k\Omega_{HN}t_3} + e^{j\Omega_C t_2^C} e^{k\Omega_{HC}t_3}]$$

$$S_2 = i0.5[e^{i(\Omega_{HN'}+\Omega_{N'})t_1} - e^{i(\Omega_{HN'}-\Omega_{N'})t_1}] \times [e^{j\Omega_N t_2^N} e^{k\Omega_{HN}t_3} + e^{j\Omega_C t_2^C} e^{k\Omega_{HC}t_3}]$$

where $\Omega_{HN'}$ and $\Omega_{N'}$ are the chemical shifts of ^1H_N and ^{15}N of NOE donors before and Ω_{HN} and Ω_N are those of NOE acceptors after the NOE mixing time, Ω_{HC} and Ω_C being the chemical shifts of ^1H_C and ^{13}C, respectively. In the F_1 dimension (the GFT NMR dimension), the terms of $\Omega_{HN'} + \Omega_{N'}$ and $\Omega_{HN'} - \Omega_{N'}$ are obtained from data $S_1 - iS_2$ and $S_1 + iS_2$, respectively. In the F_2 dimension (the TS dimension), the resonances (Ω_N, Ω_{HN}) and (Ω_C, Ω_{HC}) are easily separated using the TS scheme [24] because Ω_{HN} and Ω_{HC} are located at different regions. Therefore, the following four spectral matrices were obtained after the data processing,

ADD of H–N–N–H: $e^{i(\Omega_{HN'}+\Omega_{N'})t_1} e^{j\Omega_N t_2^N} e^{k\Omega_{HN}t_3}$,
SUB of H–N–N–H: $e^{i(\Omega_{HN'}-\Omega_{N'})t_1} e^{j\Omega_N t_2^N} e^{k\Omega_{HN}t_3}$,
ADD of H–N–C–H: $e^{i(\Omega_{HN'}+\Omega_{N'})t_1} e^{j\Omega_C t_2^C} e^{k\Omega_{HC}t_3}$,
SUB of H–N–C–H: $e^{i(\Omega_{HN'}-\Omega_{N'})t_1} e^{j\Omega_C t_2^C} e^{k\Omega_{HC}t_3}$.

Information from two 4D spectra, 4D H–N–N–H and H–N–C–H NOESY, is involved in the four sets of 3D data in a RD manner.

The (4,3)D H–N–*CN*–H NOESY experiment was performed on an 800 MHz spectrometer with a TXI room temperature probe of z-gradient for a sample of 1.4 mM $^{13}C/^{15}N$-ubiquitin in 0.5 mL 50 mM potassium phosphate, 95% H_2O–5% D_2O, pH 5.8. The total acquisition time was 48 h. The projections of the GFT-TS (4,3)D H–N–*CN*–H NOESY spectra along F_2 dimension show the distribution of the NOE peaks in the spectra (Fig. 2). SPARKY [32] and in-house developed automation procedures for GFT NMR data (Fig. 3) were used for the data analysis. The interpretation of the GFT-TS (4,3)D H–N–*CN*–H NOESY spectra is straightforward and the representative 2D planes and 1D traces are plotted in Fig. 4. For the HN and N shared dimension of the GFT-NMR data, two connected peaks (a doublet) in the F_1 dimension are symmetrical to $\Omega_{HN'}$ and separated by $\Omega_{N'}$ from the central position (Figs. 3 and 4). The chemical shifts of $\Omega_{HN'}$ and $\Omega_{N'}$ can be obtained using the doublet in spectra ADD (frequency: $\Omega_{HN'} + \Omega_{N'}$) and SUB (frequency: $\Omega_{HN'} - \Omega_{N'}$) and central peak (frequency: $\Omega_{HN'}$) in REF (a reference spectrum). In this work, the REF spectrum is 3D TS H–*CN*–H NOESY [24]. This experiment exhibits the same but less resolved NOE cross peaks as compared with the (4,3)D H–N–*CN*–H NOESY. For the *CN* dimension of the TS NMR data, the frequencies of ^{13}C or ^{15}N are well separated in F_2 and bond connectivities involved in the F_2 (^{13}C or ^{15}N) and F_3 (^1H_C or ^1H_N) dimensions provide spectral resolution for the NOE signals.

Examples are demonstrated in Fig. 4, in which the (4,3)D H–N–*CN*–H NOESY encodes proton chemical shifts in the F_1 and F_3 dimensions edited with ^{13}C or ^{15}N chemical shifts to enhance spectral resolution. The GFT NMR ADD and SUB spectra in the Fig. 4a and c show NOEs from HN_i to HN_j (i and j are residue numbers), where the HN_i correlates to N_i in the GFT NMR F_1 dimension and HN_j correlates to N_j in the TS F_2 and F_3

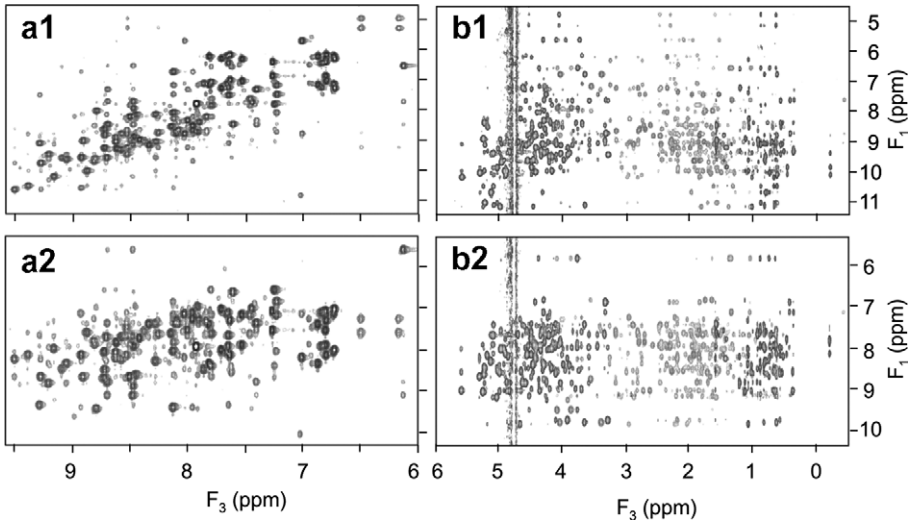

Fig. 2. Projections of the GFT-TS NOESY along F_2 (^{15}N and ^{13}C) dimension: (a1, a2) (4,3)D H–N–N–H and (b1, b2) (4,3)D H–N–C–H NOESY. (a1) and (b2) are from ADD, and (a2) and (b2) are from SUB spectra, respectively. In (b1) and (b2), there is no diagonal peak because the NOEs are created between ^1H_N and ^1H_C. The chemical shifts in the F_1 dimension displayed are scaled with respect to ^1H.

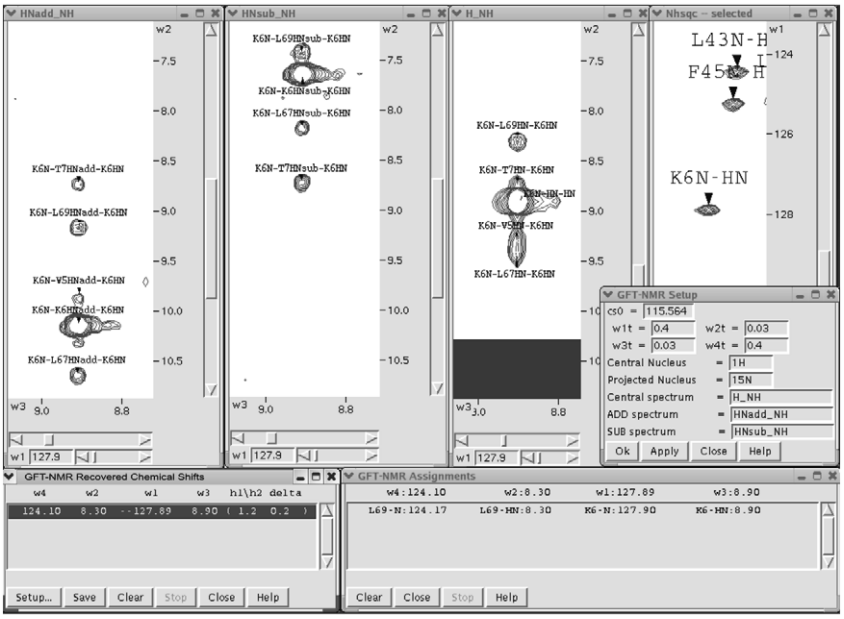

Fig. 3. The new assignment interface of SPARKY using a new extension (gft.py) for the GFT-TS (4,3)D H–N–N–H NOESY. The new extension can be used to automatically search the doublets matched with a selected central peak, recover the chemical shifts, and assign the three peaks simultaneously. The procedure is described in detail below. (1) SPARKY opens three 3D spectra: ADD, SUB, and REF. Here HNadd_NH, HNsub_NH, and H_NH are the ADD, SUB and REF, respectively. The spectra HNadd_NH and HNsub_NH are from the (4,3)D H–N–N–H NOESY. The spectrum H–NH is from the TS H–*CN*–H NOESY. (2) If a peak in the REF spectrum is selected, the extension gft.py will search the peak lists in spectra ADD and SUB. If two peaks (one in ADD and the other in SUB) are symmetrical about the selected central peak in REF, the three peaks will be used to recover the chemical shifts $\Omega_{HN'}$ and $\Omega_{N'}$ and at the same time all matched peaks under certain tolerances specified in the Setup Dialog are listed in the box of "GFT NMR Recovered Chemical Shifts". (3) If a line in the box of "GFT NMR Recovered Chemical Shifts" is selected, the related three matched peaks will be highlighted, and at the same time the extension gft.py searches the assigned resonance table and the suggested assignments are listed in the box of "GFT NMR assignment". (4) If one line in this box is selected, the assignments of the three peaks are displayed and written to the *.save file of the three spectra. Using the extended SPARKY, the GFT-TS-NOESY data can be easily analyzed. The chemical shifts in the F_1 dimensions of the GFT spectra are scaled with respect to ^{1}H.

dimensions. The 1D traces show that the peaks are unambiguously assigned to the NOEs linking K6HN to L67HN, V5HN, L69HN, and T7HN (peaks 1, 3, 4, and 5), respectively. Peak 2 is the diagonal peak of K6HN. The long range NOEs, such as K6HN to L67HN and L69HN, identified in the (4,3)D NOESY are particularly important for structure determination. In comparison, peaks 3, 4, and 5 in 1D trace from 3D TS H-*CN*-H NOESY (Fig. 4c), show severe overlaps and their assignments were ambiguous: peak 3 (9.31 ppm) could be V5HN (9.31 ppm) and/or E64HN (9.31 ppm); peak 4 (8.30 ppm) could be I3HN (8.30 ppm), I30HN (8.28 ppm), and/or L69HN (8.30 ppm); and peak 5 (8.75 ppm) could be T7HN (8.75 ppm), T14HN (8.75 ppm), L15HN (8.73 ppm), and/or T66HN (8.75 ppm). These peaks in the 3D TS H–*CN*–H NOESY cannot be unambiguously assigned without using several other NMR spectra or referencing a rough 3D structure.

In the other examples shown in Figs. 4b and d, the GFT NMR ADD and SUB spectra show resolved NOEs from HN_i to HC_j. Similar to the spectra shown in Figs. 4a and c, the HN_i correlates to N_i in the GFT NMR F_1 dimension and HC_j correlates to C_j in the TS F_2 and F_3 dimensions. The 1D traces show that the peaks are unambiguously assigned to the NOEs linking K48HB# to Q49HN, Q49HE1, Q49HE2, and K48HN (peaks 1–4, Fig. 4b), respectively, and the three more NOEs from I3N–HN–Q2CG–HG2, Q2N–HN–Q2CG–HG2 and V5N–HN–V5CB–HB, respectively. In comparison, the assignments of peaks 1, 4, 5, and 6 in 1D trace from the 3D TS H–*CN*–H NOESY (Fig. 4d), were ambiguous: the peak 1 (8.63 ppm) could be Q49HN (8.63 ppm), F4HN (8.61 ppm), T12HN (8.65 ppm) and/or E18HN (8.65 ppm); the peak 4 (7.98 ppm) could be K48HN (7.98 ppm), A28HN (7.98 ppm), G76HN (7.95 ppm) and/or D32HN (8.02 ppm); the peak 5 (8.30 ppm) could be I3HN (8.30 ppm), I30HN (8.29 ppm) and/or L69HN (8.30 ppm); the peak 6 (8.93 ppm) could be Q2HN (8.93 ppm), K6HN (8.90 ppm) and/or V17HN (8.93 ppm). However, we can unambiguously assign these peaks with the (4,3)D H–N–*CN*–H NOESY.

A similar work, in which a GFT NOESY experiment, (4,3)D [HC^{ali}/HN]-NOESY-[CH^{ali}/NH] was described, was found in literature[25]. There are differences in the methods described by Shen et al. [25] and our own [33]. In the work of Shen et al., the NOESY experiment encoded two sub-spectra, containing the information of 4D $^{15}N/^{15}N$-, $^{13}C^{alipahtic}/^{15}N$-, and $^{13}C^{aliphatic}/^{13}C^{aliphatic}$-resolved [^{1}H,^{1}H]-NOESY. This NOESY experiment provides more information than the (4,3)D H–N–*CN*–H NOESY, however, we consider that the evolutions of HN in the t_1 dimension in the work of Shen et al. are not optimized in sensitivity and resolution. First, the *J* couplings

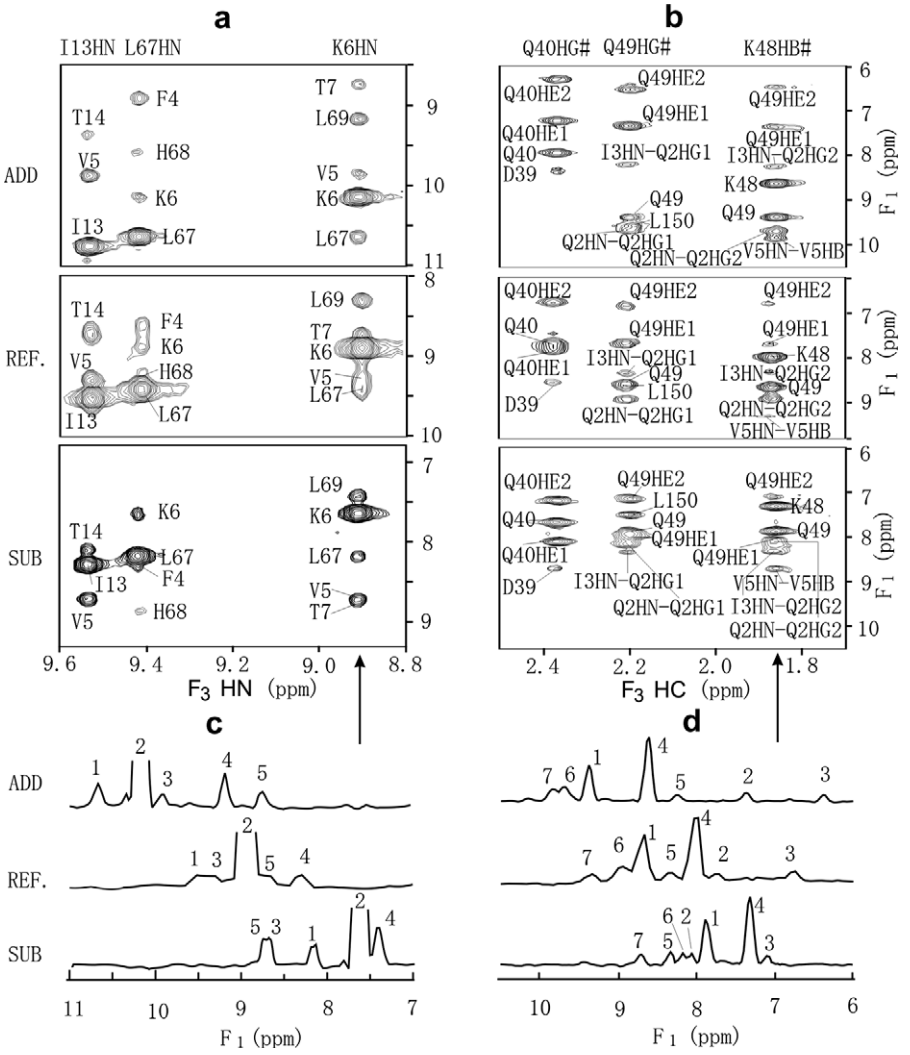

Fig. 4. 2D and 1D trace displays of (4,3)D H–N–*CN*-H NOESY along with its reference spectrum 3D TS H–*CN*–H NOESY. The small regions of 2D planes were taken at $\Omega_N = 127.90$ ppm (a) and $\Omega_C = 34.50$ ppm (b) of F_2 dimension from the (4,3)D H–N–*CN*–H NOESY and its reference spectrum. The 1D traces (c and d) were obtained from the corresponding 2D planes at the arrow positions. In (a) and (b), the NOE donors are given in the spectra and the acceptors are given at the tops of the spectra. For example, the peak at the left upper-most position in the ADD of (a) is from NOE T14N–HN–I13N–HN, and the peak at the right upper-most position in the ADD of (b) is from NOE Q49CE–HE2–K48CB–HB#. In (c), peaks 1–5 are NOE correlations linking K6HN to L67HN, K6HN (diagonal peak), V5HN, L69HN, and T7HN, respectively. In (d), peaks 1–4 are NOE correlations linking K48HB# to Q49HN, Q49HE1, Q49HE2, and K48HN, respectively. The peaks 5–7 in (d) are from NOEs I3N–HN–Q2CG–HG2, Q2N–HN–Q2CG–HG2, and V5N–HN–V5CB–HB, respectively. (4,3)D H–N–*CN*–H NOESY data acquisition used spectral widths 5601.3, 2270.5, and 4829.1, and 11160.7 Hz for H and N (t_1), C and N (t_2^C and t_2^N), and H (t_3) resonances, acquisition times 11.4, 12.8, and 6.0, and 91.8 ms, 256 and 64 increments for t_1 and t_2 dimensions, respectively, and 8 scans for each FID. 3D H–*CN*–H NOESY data acquisition used spectral widths 8802.0 (t_1), 2270.5 and 4829.1 (t_2^C and t_2^N), and 11160.7 Hz (t_3), acquisition times 9.1, 12.8 and 6.0, and 91.8 ms, 160 and 60 increments for t_1 and t_2 dimensions, respectively, and 8 scans for each FID. An AU program gftnoe and a macro gftnoe.M were written to sort the data in XWINNMR and NMRPIPE [34], respectively. Data analyzing software SPARKY [32] was extended for the analysis of the new GFT-TS (4,3)D H–N–*CN*–H NOESY data. The chemical shifts in F_1 dimension displayed are scaled with respect to ^1H.

($^1J_{^{15}N-\ ^{13}CA} = 7$–$11$ Hz, $^2J_{^{15}N-\ ^{13}CA} = 4$–$9$ Hz) between ^{15}N and $^{13}C_\alpha$ during $\kappa \times t_1$ were not removed, which result in the loss of signal intensity (5% on average, from the comparison of experimental data). Second, a scaling factor κ of 0.5 was used, which decreases the resolution of ^{13}C and ^{15}N resonances compared with that of $^1H_{ali}$ and ^1H_N in the projected dimension. Third, a large spectral width, 12,500 Hz (from Table 2 of reference 25) on a 600 MHz NMR spectrometer, was used for the projected dimension, which either further reduces the digital resolutions of ^1H_N and ^{15}N in the projected dimension or increases the number of FIDs in t_1 dimension, and reduces the speed of data acquisition. In comparison, the spectral width for HN in (4,3)D H–N–*CN*–H NOESY described in this work is only about 4200 Hz (=5600*6/8) on a 600 MHz NMR spectrometer. Therefore, the potential ^1H_N and ^{15}N's digital resolutions in the projected dimension of the (4,3)D H–N–*CN*–H NOESY are 3-times higher than that of the (4,3)D [HC^{ali}/HN]-NOESY-[CH^{ali}/NH] for same number of data points acquired. Finally, the resonance dispersion

in the sub spectrum for $\Omega_{HC} - \kappa\Omega_C$ is decreased compared with a normal spectrum. This is because the resonance frequency Ω_{HC} of ^1H_C is normally increased as the resonance frequency Ω_C of ^{13}C, and the subtraction decreases the separations of resonant peaks, again reducing resolution. However, there is no such relationship between Ω_{HN} and Ω_N as Ω_{HC} and Ω_C, the dispersion in the sub spectrum of $\Omega_{HN} - \kappa\Omega_N$ is thus unaffected.

We also consider that the data generated from (4,3)D HC^{ali}–HC^{ali} NOESY in the (4,3)D [$\underline{HC}^{ali}$/$\underline{HN}$]-NOESY-[CH^{ali}/NH] are not essential for structure determination. This is because that the 3D $^{13}C/^{15}N$ separated H–*CN*–H NOESY [18–24] would contain more NOE distances than those detected from (4, 3)D NOESY due to its low sensitivity and resolution. In our method, we can use the NOE distance constraints from the (4,3)D $\underline{H}$–$\underline{N}$–*CN*–H NOESY of higher resolution to build up the tertiary folding of proteins, and use this information to guide the assignment of NOEs from 3D $^{13}C/^{15}N$ separated H–*CN*–H NOESY, and then apply all NOE distance constraints to further improve the calculated structure. Overall, our experiment is optimized for the detection of $\underline{HN}$ in the projected dimension, which has better sensitivity and resolution than the counterpart although it provides less information. Therefore, the two methods are complementary in serving different needs and the work described herein is a suitable choice when higher sensitivity and resolution rather than more connectivities are required.

The (4,3)D $\underline{H}$–$\underline{N}$–*CN*–H NOESY provides a fast approach to acquire two 4D NOESY data, but it sacrifices sensitivity as all GFT experiments. The sensitivity of the (4,3)D $\underline{H}$–$\underline{N}$–*CN*–H NOESY is about 1/2.3-time (average for five pairs of randomly selected peaks. The different experimental times are already considered) of that of the 3D H–*CN*–H NOESY. One part of the sensitivity reduction is from the intrinsic $\sqrt{2}$-time sensitivity loss of all GFT experiments and the other part is mainly from the increased length of pulse sequence of the (4,3)D $\underline{H}$–$\underline{N}$–*CN*–H NOESY compared with the 3D H–*CN*–H NOESY. However the (4,3)D $\underline{H}$–$\underline{N}$–*CN*–H NOESY has same pulse sequence length as a standard 4D HSQC–NOESY–HSQC, and they have same signal decay from relaxation. Therefore, the theoretical sensitivity of (4,3)D $\underline{H}$–$\underline{N}$–*CN*–H NOESY is $1/\sqrt{2}$-time of that of the standard 4D HSQC–NOESY–HSQC.

We demonstrated a GFT-TS NMR experiment that is available for simultaneously recording multiple 4D NOESY spectra of a protein in a time period and with improved spectral resolution that are comparable to 3D NOESY. The availability of the NOESY experiments of this type has important implications in the acceleration of protein structure determination and the improvement in quality of structures derived from NMR spectroscopy. For instance, we showed that many long range NOEs, in addition to short range NOEs, can be easily, unambiguously assigned in the (4,3)D $\underline{H}$–$\underline{N}$–*CN*–H NOESY. Long range NOEs are critical for building the correct tertiary folding of proteins. Ubiquitin (1D3Z.pdb) contains 28 long range ^1H_N–^1H_N NOEs with $|i - j| \geqslant 5$ (i and j are residue numbers) and $d_{HH} < 4.5$ Å (d_{HH} is the interproton distance). In the sub-spectrum, (4,3)D $\underline{H}$–$\underline{N}$–N–H NOESY, all 28 NOEs were detected, although three of these NOE assignments may be ambiguous due to their intrinsic overlapping of resonances. Even real 4D spectra cannot resolve this kind of ambiguity. A useful feature in the other sub-spectrum, (4,3)D $\underline{H}$–$\underline{N}$–C–H NOESY, is the absence of strong diagonal peaks (Figs. 2b1 and b2) and thus more cross peaks are discernable. The GFT-TS (4,3)D NOESY was obtained with 48-hour experimental time using the sample of 1.4 mM protein, representing a 5- or 2.5-fold reduction of experimental time compared with that of two 4D H–N–N–H and H–N–C–H NOESY, which require nearly 10 or 5 days of experimental time if the two 4D data are acquired separately or together in a time-shared mode. As with the (4,3)D [$\underline{HC}^{ali}$/$\underline{HN}$]-NOESY-[CH^{ali}/NH], a 3D H–*CN*–H NOESY of one day experimental time is needed to provide the reference spectrum for the (4,3)D NOESY spectra. However, the 3D H–*CN*–H NOESY serves a dual purpose of providing the reference for the (4,3)D NOESY and also providing a ^{13}C-separated 3D NOESY. Even upon including the 3D H–*CN*–H NOESY into the (4,3)D NOESY experiment, this set of experiments still represents a 3.3- or 1.7-fold reduction of the experiment time.

A practical aspect of the usefulness of the method is in the availability of utility scripts for GFT-TS data processing and analyzing so that the data can be easily assigned, compared with other conventional experimental data sets, and used for structure determination. The software package containing pulse sequences, macros and scripts for (1) data acquisition using a Bruker NMR spectrometer; (2) data processing using XWINNMR and NMRPIPE; and (3) data analysis using SPARKY, is available at www.bchs.uh.edu/~kecknmr. Together the (4,3)D $\underline{H}$–$\underline{N}$–*CN*–H GFT-TS NOESY pulse sequence and the tools for data processing and analysis reported herein will find applications for structural studies and efficient three-dimensional structure determination of small to medium sized proteins.

Acknowledgments

The 800 MHz NMR spectrometer at the Keck/IMD NMR Center at the University of Houston is funded by the W. M. Keck Foundation and the University of Houston. This research was in part supported by grants from NIH (R42 GM067364) and the Robert A. Welch Foundation (E-1027).

References

[1] Ē. Kupče, R. Freeman, J. Biomol. NMR 27 (2003) 383–387.
[2] Ē. Kupče, R. Freeman, J. Am. Chem. Soc. 126 (2004) 6429–6440.
[3] E. Kupče, R. Freeman, J. Magn. Reson. 173 (2005) 317–321.
[4] S. Kim, T. Szyperski, J. Am. Chem. Soc. 125 (2003) 1385–1393.

[5] B. Bersch, E. Rossy, J. Covès, B. Brutscher, J. Biomol. NMR 27 (2003) 57–67.
[6] W. Koźmiński, I. Zhukov, J. Biomol. NMR 26 (2003) 157–166.
[7] Y. Xia, G. Zhu, S. Veeraraghavan, X. Gao, J. Biomol. NMR 29 (2004) 467–476.
[8] H.S. Atreya, T. Szyperski, Proc. Natl. Acad. Sci. USA 101 (2004) 9642–9647.
[9] T. Szyperski, G. Wider, J.H. Bushweller, K. Wüethrich, J. Am. Chem. Soc. 115 (1993) 9307–9308.
[10] B. Brutscher, J.P. Simorre, M.S. Caffrey, D. Marion, J. Magn. Reson. B 105 (1994) 77–82.
[11] B. Brutscher, F. Cordier, J.P. Simorre, M.S. Caffrey, D. Marion, J. Biomol. NMR 5 (1995) 202–206.
[12] F. Löhr, H. Rüterjans, J. Biomol. NMR 6 (1995) 189–197.
[13] K. Ding, A.M. Gronenborn, J. Magn. Reson. 156 (2002) 262–268.
[14] T. Szyperski, D.C. Yeh, D.K. Sukumaran, H.N.B. Moseley, G.T. Montelione, Proc. Natl. Acad. Sci. USA 99 (2002) 8009–8014.
[15] Y. Xia, C.H. Arrowsmith, T. Szyperski, J. Biomol. NMR 24 (2002) 41–50.
[16] S. Hiller, F. Fiorito, K. Wüthrich, G. Wider, Proc. Natl. Acad. Sci. USA 102 (2005) 10876–10881.
[17] L. Frydman, T. Scherf, A. Lupulescu, Proc. Natl. Acad. Sci. USA 99 (2002) 15858–15862.
[18] S.M. Pascal, D.R. Muhandiram, T. Yamazaki, J.D. Forman-Kay, L.E. Kay, J. Magn. Reson. 103 (1994) 197–201.
[19] B.T. Farmer II, L. Mueller, J. Biomol. NMR 4 (1994) 673–687.
[20] H. Vis, R. Boelens, M. Mariani, R. Stroop, C.E. Vorgias, K.S. Wilson, R. Kaptein, Biochemistry 33 (1994) 14858–14870.
[21] M. Sattler, J. Schleucher, C. Griesingner, Prog. Nucl. Magn. Reson. 34 (1999) 93–158.
[22] R. Jerala, G.S. Rule, J. Magn. Reson. B 108 (1995) 294–298.
[23] Y. Xia, D. Man, G. Zhu, J. Biomol. NMR 19 (2001) 355–360.
[24] Y. Xia, A. Yee, C.H. Arrowsmith, X. Gao, J. Biomol. NMR 27 (2003) 193–203.
[25] Y. Shen, H.S. Atreya, G. Liu, T. Szyperski, J. Am. Chem. Soc. 127 (2005) 9085–9099.
[26] G.M. Clore, A.M. Gronenborn, Science 252 (1991) 1390–1399.
[27] G.W. Vuister, G.M. Clore, A.M. Gronenborn, R. Powers, D.S. Garrett, R. Tchudin, A. Bax, J. Magn. Reson. 101 (1993) 210–213.
[28] L.E. Kay, G.M. Clore, A. Bax, A.M. Gronenborn, Science 249 (1990) 411–414.
[29] A. Bax, Curr. Opin. Struct. Biol. 4 (1994) 738–744.
[30] M. Sattler, M. Maurer, J. Schleucher, C. Griesinger, J. Biomol. NMR 5 (1995) 97–102.
[31] G. Zhu, Y. Xia, D. Lin, X. Gao, Methods Mol. Biol. 278 (2004) 57–78.
[32] T.D. Goddard, D.G. Kneller, SPARKY 3. University of California, San Francisco.
[33] The first submission of this work to J. Am. Chem. Soc. was in November 23, 2004, which predates the submission of the publication by Shen et al. (reference #25). This establishes that our work was accomplished independently.
[34] F. Delaglio, S. Grzesiek, G.W. Vuister, G. Zhu, J. Pfeifer, A. Bax, J. Biomol. NMR 6 (1995) 277–293.